

A Novel Copper(I/II) Oxophosphate Chloride with a Quasi-One-Dimensional μ_4 -Oxo-Bridged Copper(II) Chain. Crystal Structure and Magnetic Properties of $[\text{Na}_2\text{Cu}^{\text{II}}_3(\text{PO}_4)_2][\text{Cu}^{\text{I}}\text{OCl}]$

Kristen M. S. Etheredge[†] and Shiou-Jyh Hwu^{*,*}

Departments of Chemistry, Rice University, P.O. Box 1892, Houston, Texas 77251, and Clemson University, Clemson, South Carolina 29634

Received December 28, 1995[⊗]

In a continuing search for mixed-valence copper phosphate compounds, crystals of a novel copper(I/II) oxophosphate chloride, $\text{Na}_2\text{Cu}_4\text{P}_2\text{O}_9\text{Cl}$, have been grown in a low-temperature eutectic flux of 23% NaCl and 77% CuCl (mp = 315 °C). The title compound crystallizes in an orthorhombic lattice, *Cmcm* (No. 63), with $a = 13.614$ (2) Å, $b = 10.385$ (2) Å, $c = 6.372$ (2) Å, and $V = 900.8$ Å³; $Z = 4$. This new compound is a welcome addition to the small family of electronically distinct copper phosphates. The extended structure exhibits an interesting quasi-one-dimensional chain consisting of fused tetrahedra of copper(II) atoms centered by a μ_4 -oxo-bridging oxygen atom. This mixed framework is composed of $[\text{Cu}(2)^{\text{II}}\text{O}_6] - [\text{Cu}(1)^{\text{I}}\text{O}_4\text{Cl}] - [\text{Cu}(3)^{\text{I}}\text{O}_2\text{Cl}_3]$ fused polyhedra. The Cu^{2+} centers are closely spaced, 3.03–3.19 Å, creating an environment conducive to a magnetic transition at ~5 K associated with the diffused antiferromagnetic coupling starting at 220 K. In this paper, the synthesis, thermal properties, and bond valence analyses of $\text{Na}_2\text{Cu}_4\text{P}_2\text{O}_9\text{Cl}$ are also addressed.

Introduction

Recently, several examples of mixed-valence, low-dimensional transition metal oxo compounds were synthesized and characterized by our research group: $\text{La}_4\text{Ti}(\text{Si}_2\text{O}_7)_2(\text{TiO}_2)_{4m}$ ($m = 1, 2$)¹ and $(\text{Ba}_3\text{Nb}_6\text{Si}_4\text{O}_{26})_n(\text{Ba}_3\text{Nb}_8\text{O}_{21})$ ($n = 1-4$) series.² In these examples, the nanosized transition metal oxide layers (sheets) and chains (wires) are structurally isolated and electronically insulated by closed-shell, nonmagnetic oxyanions, specifically, $\text{Si}_2\text{O}_7^{6-}$. These types of structures are of particular interest for investigating the magnetic interactions of delocalized electrons in a confined transition metal oxide lattice.

In depth research into copper phosphate chemistry via molten-salt synthesis has proven to be productive in discovering novel structures with interesting magnetic properties.^{3,4} Prior to these studies, a large collection of copper-based phosphate compounds were reported in the literature, as cited in ref 3a, but these compounds generally exhibit extended three-dimensional structures containing isolated $\text{Cu}^{\text{II}}\text{O}_n$ ($n = 4-6$) polyhedra. Low-dimensional copper oxide frameworks and/or mixed-valence copper compounds are rare. To our knowledge, in the Cu(I/II) system, only one phosphate, Cu_2PO_4 ,⁴ and one arsenate, $\text{Pb}_2\text{Cu}_8(\text{AsO}_4)_6$,⁵ are known. The former has an attractive extended framework which consists of low-dimensional arrays of nearly parallel $\text{Cu}^{\text{I}}\text{O}_2$ linear units and short $\text{Cu}^{\text{I}}-\text{O}-\text{Cu}^{\text{II}}-\text{O}-\text{Cu}^{\text{I}}$ and $\text{Cu}^{\text{II}}-\text{O}-\text{Cu}^{\text{II}}$ linkages. The $\text{Cu}^{\text{I}}\text{O}_2$ units are closely spaced, 2.74 Å, due to cross-linking by the PO_4 tetrahedra; the short

Cu–O linkages are connected by long $\text{Cu}^{\text{II}}-\text{O}$ bonds. The magnetic data show antiferromagnetic ordering below 170 K.

This research has been extended to include electropositive cations, specifically alkali and alkaline earth metals, in hopes that they will promote new framework formation. The title compound, $\text{Na}_2\text{Cu}_4\text{P}_2\text{O}_9\text{Cl}$, has been isolated from a reaction using $\text{Na}_4\text{P}_2\text{O}_7$ as a precursor in a eutectic halide flux media. Its extended structure exhibits an interesting quasi-one-dimensional framework of interconnected chains composed of $[\text{Cu}^{\text{II}}\text{O}_6] - [\text{Cu}^{\text{I}}\text{O}_4\text{Cl}] - [\text{Cu}^{\text{I}}\text{O}_2\text{Cl}_3]$ fused polyhedra. The synthesis, structure, and thermal and magnetic properties of this sodium copper(I/II) oxophosphate chloride are reported.

Experimental Section

Synthesis. Single crystals of $\text{Na}_2\text{Cu}_4\text{P}_2\text{O}_9\text{Cl}$ were grown from a reaction mixture containing $\text{Na}_4\text{P}_2\text{O}_7$ (from $\text{Na}_4\text{P}_2\text{O}_7 \cdot 10\text{H}_2\text{O}$, Mallinckrodt, 99.5%, dried at 100 °C in air for several hours) and CuO (Strem, 99.9999%) with the nominal composition of $\text{Na}_4\text{Cu}_4\text{P}_2\text{O}_{11}$. The mixture was loaded into a eutectic flux of 23% NaCl (EM Science, 99.9%) and 77% CuCl (Aldrich, 99+%), mp = 315 °C, with a flux to charge ratio of 5:1. The starting materials and flux were ground, placed in a carbon-coated silica ampule, heated to 500 °C for 4 days, cooled at 2 °C/h to 300 °C, and then cooled quickly (50 °C/h) to room temperature. Brownish-green crystals of the title compound were isolated by washing the reaction product with deionized water using a suction filtration method. A parallel reaction using KPO_3 and KCl/CuCl flux produced a known phosphate, KCuPO_4 ; no chloride inclusion was observed.

Structure Determination. A chunky, hexagonal column crystal was mounted on a glass fiber for single-crystal X-ray diffraction study. The diffraction data were collected at room temperature on a Rigaku AFC5S four-circle diffractometer. Crystallographic data for the title compound are summarized in Table 1. The unit cell parameters and the orientation matrix for data collection were determined by a least-squares analysis of 25 peak maxima with $7^\circ < 2\theta < 21^\circ$. There was no detectable decay during data collection, according to the intensities of three standard reflections (–2,0,–2; –2,0,0; –2,2,0) which were measured every 150 reflections. Lorentz–polarization and empirical absorption corrections based on three computer-chosen azimuthal scans ($2\theta = 5.99, 18.02, 24.11^\circ$) were applied to the intensity data; Friedel pairs were

[†] Rice University.

^{*} Clemson University.

[⊗] Abstract published in *Advance ACS Abstracts*, August 1, 1996.

- (1) (a) Wang, S.; Hwu, S.-J. *J. Am. Chem. Soc.* **1992**, *114*, 6920. (b) Wang, S.; Hwu, S.-J. *Inorg. Chem.* **1995**, *34*, 166. (c) Wang, S.; Hwu, S.-J.; Paradis, J. A.; Whangbo, M.-H. *J. Am. Chem. Soc.* **1995**, *117*, 5515. (d) Wang, S. Ph.D. Dissertation, Rice University, 1993.
- (2) (a) Serra, D. L.; Hwu, S.-J. *J. Solid State Chem.* **1992**, *101*, 32. (b) Serra, D. L., Ph.D. Dissertation, Rice University, 1993.
- (3) (a) Etheredge, K. M. S.; Hwu, S.-J. *Inorg. Chem.* **1995**, *34*, 1495. (b) Etheredge, K. M. S.; Hwu, S.-J. *Inorg. Chem.* **1995**, *34*, 3123. (c) Etheredge, K. M. S.; Hwu, S.-J. *Inorg. Chem.* **1996**, *35*, 1474.
- (4) Etheredge, K. M. S.; Hwu, S.-J. *Inorg. Chem.* **1995**, *34*, 5013.
- (5) Effenberger, H. *J. Solid State Chem.* **1995**, *114*, 413.

Table 1. Crystallographic Data for Na₂Cu₄P₂O₉Cl

empirical formula	Na ₂ Cu ₄ P ₂ O ₉ Cl	space group	<i>Cmcm</i> (No. 63)
fw	541.53	<i>T</i> , °C	23
<i>a</i> , Å	13.614(2)	<i>λ</i> , Å	0.710 69
<i>b</i> , Å	10.385(2)	ρ_{calcd} , g cm ⁻³	3.993
<i>c</i> , Å	6.372(2)	linear abs	96.800
<i>V</i> , Å ³	900.8(4)	coeff, cm ⁻¹	
<i>Z</i>	4	<i>R</i> ₁ ^a	0.029
		<i>wR</i> ₂ ^b	0.085

^a $R_1 = \sum[|F_o| - |F_c|]/\sum|F_o|$. ^b $wR_2 = [\sum\{w(F_o^2 - F_c^2)\}^2/\sum\{w(F_o^2)\}^2]^{1/2}$, with $w = [\sum F_o^2 + (aP)^2 + bP]^{-1}$ and $P = 0.33F_o^2 + 0.67F_c^2$.

merged. The TEXSAN software package⁶ was used for crystal structure solution. On the basis of extinction conditions and correct structure solution, space group *Cmcm* (No. 63) was unambiguously chosen. Atomic coordinates of Na, Cu, P, and Cl were determined using the SHELX-86 program,⁷ and those of oxygen atoms were resolved by successive least-squares refinements on *F*² using SHELXL-93.⁸ Initially, the structure was refined by fixing the Cu(3) atom at the special position 4c (0, *y*, 1/4; *y* = 0.3737(1)), with *R*₁ = 0.033, *wR*₂ = 0.090, and GOF = 1.21. A large thermal parameter, *U*_{eq} = 0.049 Å², for Cu(3) led to a further investigation of the structure. A model containing disorder, with respect to the Cu(3) site, was introduced and the new refinement was based on the 8f (0, *y*, *z*) site by allowing the *z* coordinate to vary with the occupancy fixed at 50%. The structural refinement gave improved *R*₁/*wR*₂/GOF (0.029/0.085/1.15). (The residual *R*₁ is calculated for refinements which were performed on *F*² and is equal to the residual *R* calculated for refinements performed against *F*.) This residual, *R*₁, is included to make comparisons with other refinement methods more convenient. This scaling is done because, due to statistical factors, the refinements on *F*² are normally 2–3 times larger than the same refinement performed on *F*.) The refinement converged and resulted in a small deviation in the *z* coordinate of Cu(3), 0.258. Consequently, there is a close, but significant, Cu(3)–Cu(3) separation distance, 0.10 Å, across the mirror plane at *z* = 1/4. This relatively minor distortion causes the thermal parameter for the new Cu(3) to remain large, 0.052. The structural and thermal parameters were refined by the full-matrix least-squares method. The structural composition was verified by wavelength dispersive spectroscopy.⁹ Table 2 lists the final positional and thermal parameters.

Thermal Analysis. Differential thermal analysis (DTA) was carried out on a DuPont 9900 thermal analysis system in the temperature range 20–800 °C. The experiment was done on selected single crystals in a sealed quartz ampule. The result indicates the title compound melts congruently at ~731 °C.

Magnetic Measurements. The magnetic susceptibility was measured using a Quantum Design SQUID MPMS-5S magnetometer. The measurements were carried out from 1.76 to 300 K in fields of *H* = 0.05 and 0.5 T, showing no field dependence over the whole temperature range. Selected single crystals (~14.4 mg) were contained in a gel capsule sample holder which was suspended in a straw from the sample translator drive. The temperature and field dependences of the susceptibility of the container were previously determined, and

Table 2. Positional and Equivalent Displacement Parameters for Na₂Cu₄P₂O₉Cl

atom	<i>x</i>	<i>y</i>	<i>z</i>	<i>U</i> _{eq} ^a , Å ²
Cu(1)	0.38477(6)	0.30352(7)	1/4	0.0109(2)
Cu(2)	0	0	0	0.0081(3)
Cu(3)	0	0.3743(2)	0.258(2)	0.052(1) ^b
Cl	1/2	0.1059(2)	1/4	0.0281(6)
P	0.1682(1)	0.2046(2)	1/4	0.0093(3)
Na	0.3064(3)	0	1/2	0.0324(1)
O(1)	1/2	0.4088(6)	1/4	0.008(1)
O(2)	0.1464(4)	0.3493(4)	1/4	0.017(1)
O(3)	0.2800(3)	0.1800(5)	1/4	0.016(1)
O(4)	0.1247(2)	0.1391(3)	0.0533(5)	0.0165(7)

^a *U*_{eq} is defined as one-third of the trace of the orthogonalized **U**_{ij} tensor. ^b The Cu(3) position is refined on an 8f (0, *y*, *z*) site with the occupancy fixed at 50%; see text.

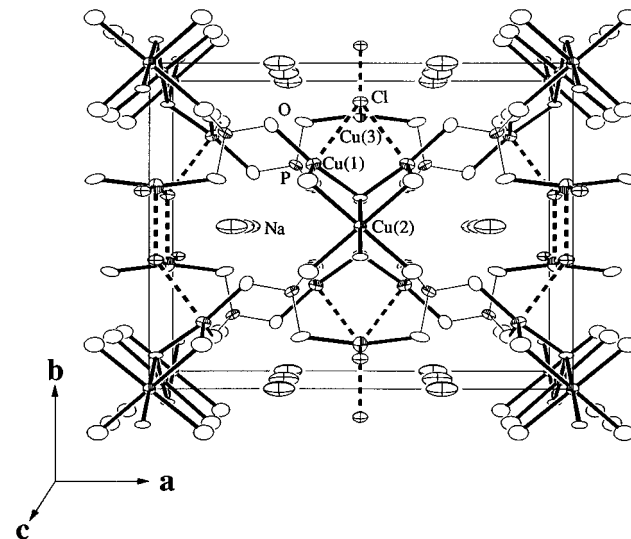


Figure 1. Perspective drawing of the Na₂Cu₄P₂O₉Cl structure projected along the *c* axis. The copper(I/II) and phosphorus geometries are highlighted with thick and thin lines, respectively. The Cu–Cl bonds are indicated by dotted lines, and Na–O bonds are eliminated for simplicity. The anisotropic thermal ellipsoids are drawn at 90% probability.

their effect was negligible. The magnetic susceptibility was corrected for core diamagnetism with Pascal's constants.¹⁰

Results and Discussion

Structure Description. Figure 1¹¹ shows a projected view of the unit cell of Na₂Cu₄P₂O₉Cl. The coordination geometries involving the copper and phosphorus cations and the oxygen and chlorine anions are highlighted, and the sodium cations reside in the channels. The copper coordination geometries can be approximated as distorted Cu(1)O₄Cl square pyramidal, Cu(2)O₆ octahedral, and Cu(3)O₂Cl₃ trigonal bipyramidal. The phosphorus atom has PO₄ tetrahedral geometry. Owing to the versatile connectivity between the polyhedra, the unit cell possesses complicated chemical bonding. This is not unusual; copper phosphates often adopt complex structures, due, in part, to the multiple coordination geometries of copper (see below). Nevertheless, the framework can be characterized as quasi-1D because of not only the channel structure but also the copper oxide chains.

The pseudo-1D copper oxide chain, as shown in Figure 2, exhibits interesting μ_4 -oxo-bridged Cu(1)₂Cu(2)₂ tetrahedra. The chains are located at the four corners and the center of the unit

(6) (a) *TEXSAN: Single Crystal Structure Analysis Software, Version 5.0*; Molecular Structure Corp.: The Woodlands, TX, 1989. (b) Cromer, D. T.; Waber, J. T. Scattering Factors for Non-hydrogen Atoms. In *International Tables for X-ray Crystallography*; Henry, N. F. M., Lonsdale, K., Eds. Kynoch Press: Birmingham, England, 1974; Vol. IV, Table 2.2A, pp 71–98.

(7) Sheldrick, G. M. In *Crystallographic Computing 3*; Sheldrick, G. M., Krüger, C., Goddard, R., Eds.; Oxford University Press: London/New York, 1985; pp 175–189.

(8) Sheldrick, G. M. SHELXL-93. University of Goettingen, Germany, 1993.

(9) WDS was run on a Cameca SX-50 with a SUN-based control and reduction system. The composition ratio of cations, Na:Cu:P = 2.26(5):3.93(5):2.07(3), approximately agrees with the structural composition. The standards used for the calibration were naturally occurring jadeite (NaAlSi₃O₆) with low levels of Ca (0.13%) and Mg (0.12%) impurities, copper metal (99.99%), and synthetic ScPO₄ (USNM 168495) for the Na, Cu, and P cations, respectively. The microprobe was run with the following parameters: 15 kV, beam current of 15 nA, beam diameter of 5 μm, and 30 s counting time.

(10) O'Connor, C. J. *Prog. Inorg. Chem.* **1982**, 29, 203.

(11) *SHELXTL PC VERS. 4.1*; Siemens Analytical X-ray Instruments Inc.: Madison, WI, 1990.

Table 3. Selected Bond Distances (Å) and Angles (deg) for Na₂Cu₄P₂O₉Cl^a

Cu(1)O ₄ Cl Square Planes			
Cu(1)—O(1) ^a	1.912(3)	Cu(1)—O(3) ^a	1.918(5)
Cu(1)—O(4) ^{b,c}	2.027(3) (2×)	Cu(1)—Cl ^a	2.583(2)
O(1) ^a —Cu(1)—O(3) ^a	172.9(2)	O(4) ^b —Cu(1)—O(4) ^c	145.0(2)
O(1) ^a —Cu(1)—O(4) ^{b,c}	83.3(1) (2×)	O(3) ^a —Cu(1)—O(4) ^{b,c}	98.6(1) (2×)
Cl ^a —Cu(1)—O(1) ^a	87.5(2)	Cl ^a —Cu(1)—O(3) ^a	85.4(1)
Cl ^a —Cu(1)—O(4) ^{b,c}	105.8(1) (2×)		
Cu(2)O ₆ Octahedra			
Cu(2)—O(1) ^{d,e}	1.853(3) (2×)	Cu(2)—O(4) ^{a,f,g,h}	2.255(3) (4×)
O(1) ^d —Cu(2)—O(1) ^e	180.0	O(1) ^{d,d,e,e} —Cu(2)—O(4) ^{a,h,f,g}	101.4(1) (4×)
O(4) ^{a,g} —Cu(2)—O(4) ^{f,h}	82.3(2) (2×)	O(1) ^{d,d,e,e} —Cu(2)—O(4) ^{f,g,a,h}	78.6(1) (4×)
O(4) ^f —Cu(2)—O(4) ^h	180.0	O(4) ^{a,f} —Cu(2)—O(4) ^{h,g}	97.7(2) (2×)
Cu(3)O ₂ Cl ₃ Polyhedra			
Cu(3)—O(2) ^{a,h}	2.011(5) (2×)	Cu(3)—Cl ⁱ	2.406(3)
Cu(3)—Cl ^j	3.237(1)	Cu(3)—Cl ^e	3.135(1)
O(2) ^a —Cu(3)—O(2) ^h	164.9(3)	Cl ⁱ —Cu(3)—O(2) ^{a,h}	97.2(1) (2×)
O(2) ^{a,h} —Cu(3)—Cl ^j	90.5(1) (2×)	O(2) ^{a,h} —Cu(3)—Cl ^e	90.5(1) (2×)
Cl ⁱ —Cu(3)—Cl ^j	88.8(3)	Cl ⁱ —Cu(3)—Cl ^e	88.8(3)
Cl ^j —Cu(3)—Cl ^e	172.3(1)		
PO ₄ Tetrahedra			
P—O(2) ^a	1.531(5)	P—O(3) ^a	1.544(5)
P—O(4) ^{a,k}	1.544(3)		
O(2) ^a —P—O(3) ^a	110.6(3)	O(2) ^a —P—O(4) ^{a,k}	111.0(2) (2×)
O(3) ^a —P—O(4) ^{a,k}	107.7(2) (2×)	O(4) ^a —P—O(4) ^k	108.6(3)

^a Symmetry transformations: (a) x, y, z ; (b) $1/2 - x, 1/2 - y, -z$; (c) $1/2 - x, 1/2 - y, 1/2 + z$; (d) $x - 1/2, y - 1/2, z$; (e) $x - 1/2, 1/2 - y, -z$; (f) $x, -y, -z$; (g) $-x, -y, -z$; (h) $-x, y, z$; (i) $x - 1/2, 1/2 + y, z$; (j) $x - 1/2, 1/2 - y, 1 - z$; (k) $x, y, 1/2 - z$.

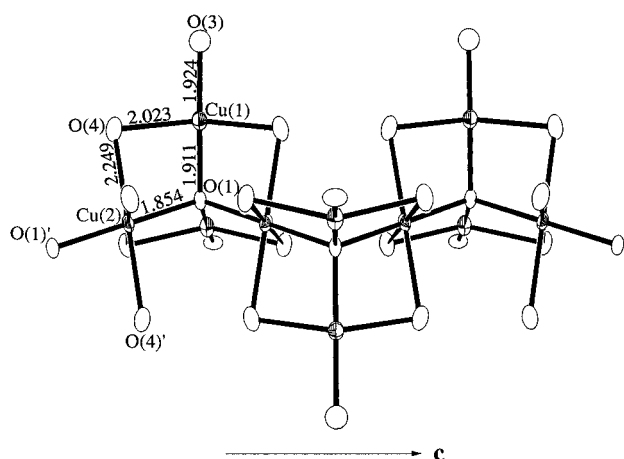


Figure 2. Partial structure of the pseudo-one-dimensional Cu(1)O₄—Cu(2)O₆ chain propagating along the *c* axis. The Cu(1)—Cl bonds are eliminated for clarity. The anisotropic thermal ellipsoids are drawn at 90% probability.

cell and run parallel to the *c* axis. Cu(2)O₆ octahedra corner-share, forming a chain along the *c* axis and are bent due to the Cu(1)O₄ unit. (The latter is the distorted square plane of the Cu(1)O₄Cl square pyramidal unit; the Cu—Cl bond has been omitted for simplicity.) A group of two Cu(1)O₄ and two Cu(2)O₆ polyhedra share a common edge, O(1)—O(4), of the polyhedra to form an attractive μ₄-O(1)-centered Cu₄ configuration. Pivoting on the oxo oxygen, a pair of Cu(1)O₄ units lean toward each other, alternating to one side or the other of the Cu(2)O₆ octahedral chain. This overall arrangement results in rather short Cu(1)—Cu(1), Cu(1)—Cu(2), and Cu(2)—Cu(2) distances, 3.14, 3.03, and 3.19 Å, respectively, corresponding to the edges of the O(1)Cu₄ tetrahedra. These Cu—Cu distances are longer than the 2.857 and 2.876 Å in Cu^{II}₄(PO₄)₂O,¹² where the short distances result from edge-shared CuO_n polyhedra and are much longer than the 2.56 Å found in elemental copper.¹³

The Cu(1) to oxygen distances lie in the range 1.91–2.03 Å (Table 3), which is comparable with the Cu(II)—O bond distances, 1.98–2.08 Å, in BaCuPO₄Cl.^{3b} Cu(1) also bonds to the Cl atom with a bond length of 2.58 Å, which is longer than 2.46 Å, the sum of the Shannon crystal radii for a 5-coordinated Cu²⁺ (0.79 Å) and Cl⁻ (1.67 Å).¹⁴ Cu(2)O₆ exhibits a Jahn—Teller distortion common to the d⁹ Cu²⁺. There are two short bonds to O(1), 1.85 Å, and four long bonds to O(4), 2.26 Å. The average of these bonds is 2.12 Å, which is close to 2.11 Å, the sum of the Shannon crystal radii for a 6-coordinated Cu²⁺ (0.87 Å) and O²⁻ (1.24 Å). This tetragonal distortion from a perfect octahedron via compressed axial oxygen atoms is rare and is formed to avoid a closer interaction with Cu(1).

A fascinating feature concerning the connectivity of two parallel chains is shown in Figure 3. The 1D chains mentioned above are interconnected through bridging Cu(3)O₂Cl₃ units, extending the framework along *b*. Each Cl is shared by two Cu(1) and one Cu(3). Cu(3) bonds to two oxygen atoms and three chlorine atoms in a trigonal bipyramidal arrangement. The distance to the two equivalent O(2) atoms is 2.01 Å, which is slightly longer than 1.98 Å, the sum of the Shannon crystal radii for Cu⁺ (0.74 Å) and O²⁻. The axial Cu—Cl bonds (dotted lines) are long, $d_{\text{Cu(3)—Cl}} = 3.24$ and 3.14 Å ($\sim c/2$, Table 3), compared to the in-plane Cu—Cl bond, 2.41 Å. The O—Cu—O bond angle is 164.9°, which is distorted from 180° due to the repulsive nature of the tightly bonded bridging Cl, 2.406 Å. This nearly linear O—Cu—O configuration has been seen for Cu(I) in the structures of Cu₂PO₄⁴ and Pb₂Cu₈(AsO₄)₆.⁶ Alternatively, the Cu(3)O₂Cl₃ unit is connected with Cu(2)O₆ via PO₄ at O(2) and O(4) (Figure 1) to extend along *b*.

The sodium cation resides in a distorted NaO₆Cl₂ environment which can be seen in Figure 4. The Na—O bond distances are

- (12) (a) Brunel-Läugt, M.; Durif, A.; Guitel, J. C. *J. Solid State Chem.* **1978**, *25*, 39. (b) Anderson, J. B.; Shoemaker, G. L.; Kostiner, E. J. *Solid State Chem.* **1978**, *25*, 49.
- (13) Greenwood, N. N.; Earnshaw, A. *Chemistry of the Elements*; Pergamon Press: Oxford, U.K., 1984; pp 1366–1368.
- (14) Shannon, R. D. *Acta Crystallogr.* **1976**, *A32*, 751.

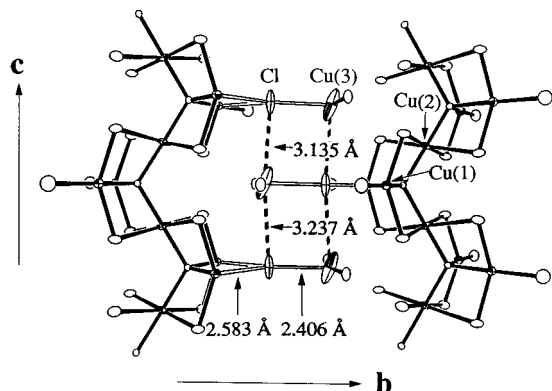


Figure 3. Two parallel Cu–O chains connected to Cu(3) cations via Cu–Cl bonds (hollow bonds). Each Cu(3) is bonded to two oxygen atoms (thick lines) and one chlorine atom in the trigonal plane and two additional chlorine atoms (dotted lines) above and below the plane to form a Cu(3)O₂Cl₃ configuration.

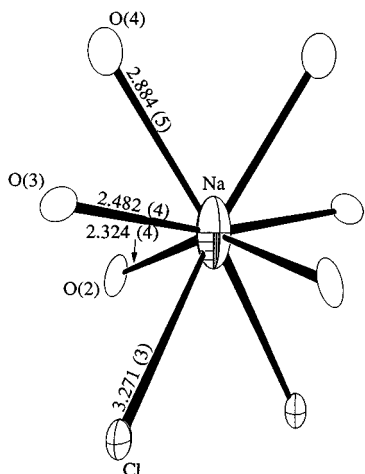


Figure 4. Drawing of the NaO₆Cl₂ geometry. The bond distances are in angstroms, and the anisotropic thermal ellipsoids are drawn at 90% probability. The unlabeled bonds are related to the labeled one by a mirror plane through the sodium atom.

quite diverse, ranging from 2.32 to 2.88 Å; this is due to the complex bond interaction occurring at each oxygen anion (O(2)/O(3)–2Na/1P/1Cu; O(4)–1P/2Cu). The average Na–O bond distance, 2.56 Å, though, is the same as 2.56 Å, the sum of the Shannon crystal radii for an 8-coordinate Na⁺ (1.32 Å) and four-coordinate O²⁻. The Na–Cl bond distances are 3.27 Å, longer than 2.99 Å, the crystal radii sum for Na⁺ and Cl⁻. With respect to the channel structure, the shortest window dimension is 3.00 Å, much shorter than 5.12 Å = 2 × 2.56 Å (Na–O distance), suggesting that Na ion conductivity is unlikely.

The bond valence sum (BVS) analyses¹⁵ indicate that Na₂Cu₄P₂O₉Cl is a mixed-valence copper(I/II) compound. The calculated charge for Cu(1) is +2.05 including the chlorine vs +1.84 excluding the chlorine. For Cu(2), a value of +2.11 is calculated. The formal oxidation state of each of these copper cations can be assigned as +2. The formal charge of the Cu(3) site can be assigned as +1 since the calculated BVS is +0.92. The Na(1) cation has a calculated charge of +0.96 based on the NaO₆Cl₂ coordination. The phosphorus charge is calculated to be +4.71, which is close to its formal charge of +5.

Magnetic Properties. Magnetic susceptibility data are plotted in Figure 5 as both molar susceptibility (χ) of Na₂Cu₄P₂O₉Cl and χT versus temperature (T). The features of the χT vs T curve can be divided into three temperature regions.

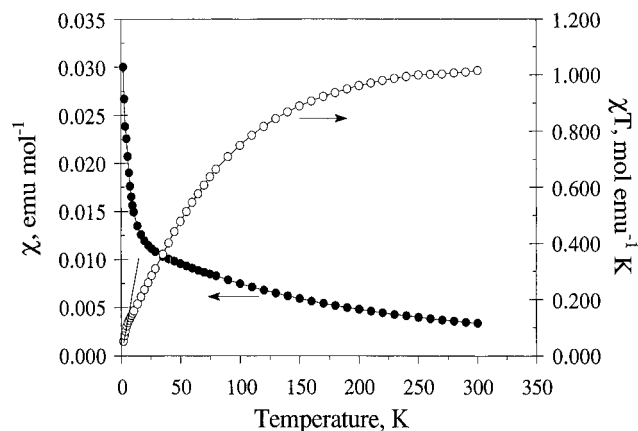


Figure 5. Susceptibility data for Na₂Cu₄P₂O₉Cl, plotted as χ and χT vs T . The solid line drawn on the χT curve helps to view the sudden change below 5 K (see text).

At the higher temperatures, ca. 220–300 K, a nearly perfect Curie–Weiss fit is possible for the magnetic data. The intermediate-temperature region, ca. 5–220 K, exhibits a gradual decrease in χT as the temperature is lowered, which indicates a weak antiferromagnetic coupling. The antiferromagnetic ordering is diffuse and starts to take place above the low end of Curie–Weiss fit, namely 220 K. Looking carefully at the low-temperature region, $T < 5$ K, we observe a rapid decrease in χT .

The high-temperature magnetic susceptibility data are fitted with the Curie–Weiss equation, $\chi = C/(T - \Theta)$, giving rise to $C = 3.77 \times 10^{-1}$ emu K/mol Cu²⁺, $\Theta = -34.3$ K. The corresponding $\mu_{\text{eff}} (=2.83\sqrt{C})$ is 1.74 μ_B , which is consistent with the spin-only ($S = 1/2$) value of 1.73 μ_B /mol of Cu²⁺. The antiferromagnetic couplings are likely induced via a commonly known superexchange mechanism¹⁶ through the Cu(1)–O(1)–Cu(2), Cu(1)–O(4)–Cu(2), and Cu(2)–O(1)–Cu(2) pathways of the μ_4 -O(1)Cu₄ core (Figure 2). The internuclear coupling constant $J_{\text{Cu}\cdots\text{Cu}}$ can be calculated on the basis of the Cu–O–Cu bridge angle, φ , within the Cu₂O₂ subunits of the core. The equation used here for the evaluation of J values is obtained from the report of the μ_4 -oxo-bridged copper(II) molecular complexes [Cu₄OX₄(mbpp)₂] ($X = \text{Cl}, \text{Br}$).¹⁷ By use of the bridging angles, 107.0, 89.9, and 118.2°, the J values are calculated to be –706, 551, and –1530 cm⁻¹, respectively. The relatively large negative J values suggest a significant antiferromagnetic coupling between the Cu²⁺ magnetic centers in the Cu(II)–O chain. A competitive coupling is probably occurring through Cu(1)–O(4)–Cu(2), since this angle is so close to 90° and a positive J value results. The combination of these three pathways and their respective couplings gives rise to the complicated magnetic properties in the low-temperature region.

It must be noted that a true fit of the experimental magnetic data is not possible due to the complexity of this system. Since the interchain connectivity is made of closed-shell ions, Cl⁻ and Cu⁺, a significant magnetic exchange contribution via this pathway has been excluded for simplicity in the above discussion. A detailed theoretical investigation is necessary to understand fully the magnetic exchange interaction in the title compound.

(16) Hay, P. J.; Thibault, J. C.; Hoffmann, R. *J. Am. Chem. Soc.* **1975**, *97*, 4884.

(17) A reviewer brought to our attention the following reference: Reim, J.; Griesar, K.; Haase, W.; Krebs, B. *J. Chem. Soc., Dalton Trans.* **1995**, 649. The equation used for the calculations is $J/\text{cm}^{-1} = -73.54\varphi + 7162$. The calculated J values are consistent with those derived from the equation reported by Hatfield et al.: Crawford, V. H.; Richardson, H. W.; Wasson, J. R.; Hodgson, D. J.; Hatfield, W. E. *Inorg. Chem.* **1976**, *15*, 2107.

(15) Brese, N.; O'Keefe, M. *Acta Crystallogr.* **1991**, *B47*, 192.

Summary

A novel mixed-valence copper(I/II) phosphate, $\text{Na}_2\text{Cu}_4\text{P}_2\text{O}_9\text{Cl}$, has been isolated via a low-temperature eutectic flux reaction of 23% NaCl and 77% CuCl (mp = 315 °C). The title compound is one of the few electronically distinct phosphates in the mixed-valence compound family and is formed by chemistry serendipity via inclusion of a CuCl/NaCl flux. The structure exhibits an exciting and rare pseudo-one-dimensional, μ_4 -oxo-bridged Cu(II) chain. The 1D Cu(II)–O chain consists of a closely spaced Cu(II) oxo structure, which is conducive to the complicated magnetic properties. The formal oxidation state assignments accomplished by the magnetic and BVS studies suggest that the title compound is a new addition of the mixed-valence copper phosphate family.

Acknowledgment. Support of this work by the National Science Foundation (Grant DMR-9208529) is gratefully acknowledged, as are funds for the Rigaku AFC5S diffractometer and the SQUID magnetometer. The authors are indebted to Mr. M. L. Pierson and Dr. Virginia B. Sisson for microprobe analysis and the reviewers for their comments concerning the interpretation of magnetic properties.

Supporting Information Available: Tables of detailed crystallographic data, anisotropic thermal parameters, and bond distances and angles (7 pages). Ordering information is given on any current masthead page.

IC9516471